Rapid, DNA-induced subunit exchange by DNA gyrase

Thomas Germe[1,2*], Natassja G. Bush[1,3], Victoria Baskerville[1], Dominik Saman[4], Justin Benesch[4] and Anthony Maxwell[1]

[1]Dept. Biochemistry & Metabolism, John Innes Centre, Norwich Research Park, Norwich NR4 7UH, UK;
[2]Present address: Dept. of Biochemistry and Molecular Genetics, University of Colorado Anschutz, 12801 E 17th Ave, CO 80045, USA.
[3]Present address: European Molecular Biology Laboratory, EMBL-European Bioinformatics Institute (EMBL-EBI), Hinxton, Cambridge, CB10 1SD, UK.
[4]Department of Chemistry, Biochemistry Building, University of Oxford, South Parks Road, Oxford, OX1 3QU, UK

*To whom correspondence should be addressed: thomas.germe@cuanschutz.edu

ABSTRACT

DNA gyrase, a ubiquitous bacterial enzyme, is a type IIA topoisomerase formed by heterotetramerisation of 2 GyrA subunits and 2 GyrB subunits, to form the active complex. GyrA is usually found as a dimer in solution, whereas GyrB can exist as a monomer. DNA gyrase is able to loop DNA around the C-terminal domains (CTDs) of GyrA and pass one DNA duplex through a transient double-strand break (DSB) established in the other duplex. This results in the conversion of a positive loop into a negative one, thereby introducing negative supercoiling into the bacterial genome, an activity essential for DNA replication and transcription. The strong protein interface in the GyrA dimer must be broken to allow passage of the transported DNA segment and it is generally assumed that the interface is usually stable and only opens when DNA is transported, to prevent the introduction of deleterious DSBs in the genome. In this paper we show that DNA gyrase can exchange its DNA-cleaving interfaces between two active heterotetramers. This so-called "subunit exchange" can occur within a few minutes in solution. We also show that bending of DNA by gyrase is essential for cleavage but not for DNA binding *per se,* and favors subunit exchange. Subunit exchange is also favored by DNA wrapping and an excess of GyrB. We suggest that proximity, promoted by GyrB oligomerization and binding and wrapping along a length of DNA, between two heteroteramers favors rapid interface exchange. This exchange does not require ATP, can occur in the presence of fluoroquinolones, and raises the possibility of non-homologous recombination solely through gyrase activity. The ability of gyrase to undergo subunit exchange also explains how gyrase heterodimers, containing a single active-site tyrosine, can carry out double-strand passage reactions.

INTRODUCTION

The genome of bacterial cells is maintained at a negative superhelical density through the combined activity of various DNA topoisomerases, enzymes that can alter the linking number between the two DNA strand constituting the bacterial genome (Vos, Tretter et al. 2011, Bush, Evans-Roberts et al. 2015). The only enzyme that can introduce negative supercoils is a type IIA topoisomerase, DNA gyrase. An active gyrase complex is constituted by 2 GyrA subunits, encoded by the *gyrA* gene, and 2 GyrB subunits, encoded by the *gyrB* gene, thus forming an A_2B_2 heterotramer (Fig. 1). The A_2B_2 complex can bind a segment of DNA (green, Fig. 1) sandwiched between the 2 TOPRIM domains of the GyrB subunits and the two tower domains of GyrA and sitting on the winged-helix domain (WHD) domain of GyrA. The enzyme is able to establish a transient double-strand break in this DNA segment through transesterification from a 5′-phosphate in the DNA backbone to a catalytic tyrosine (Y122 in *Escherichia coli* gyrase, Fig. 1). The DNA duplex that extends from the cleaved segment can wrap in a positive loop around the GyrA C-terminal domains (CTDs) and the other extremity of the loop can be passed through the various interfaces of the enzyme, including the DNA break, thereby converting the positive wrap into a negative one, and resulting in the introduction of negative supercoils once the DNA break has been re-sealed. Therefore, gyrase needs to be able to transport a DNA duplex through the whole enzyme, i.e, three interfaces (Fig. 1). The first one is constituted by the ATPase domain at the N-terminus of GyrB, whose dimerization is controlled by the binding of two ATPs and results in the trapping of the transported DNA (T) segment that enters through the open interface. This interface is dubbed the N-gate. The transport of DNA is coupled to the binding and hydrolysis of ATP. The second interface the duplex must go through is the DNA gate, which is constituted by the DNA break itself and a protein-protein interface between the two GyrA subunits (WHD domains). The duplex can then exit the enzyme through the C-gate (Fig. 1). There must be some coupling between the interfaces opening and closing since opening them all at the same time would cause the enzyme to come apart and the formation of a permanent double-stranded break (DSB). This is never observed at any detectable level with the purified enzyme *in vitro.*
It has been suggested that the coupling between ATP binding and hydrolysis acts as a safety mechanism by only allowing DNA transport through the DNA gate and C-gate when the ATP interface (N-gate) is closed (Bates and Maxwell 2007). However, gyrase can perform strand passage without ATP (and therefore with the N-gate opened), without introducing DSBs (Gellert, Mizuuchi et al. 1977, Sugino, Peebles et al. 1977), suggesting that some allosteric coupling prevents the DNA gate and the C-gate from being opened at the same time. Consistent with this, the purified GyrA subunit forms stable dimers in solution, whereas the GyrB subunit can be observed as a monomer (see results) in the absence of ATP (Costenaro, Grossmann et al. 2007). While the N-gate is controlled by ATP, it is unclear what controls the opening of the DNA gate and the C-gate. However, clear structural evidence obtained mainly with eukaryotic topoisomerase II suggests coupling between motion of the WHD domains and the opening of

the C-gate, pointing to a coordination between DNA cleavage status and the opening of the C-gate (Dong and Berger 2007, Wendorff, Schmidt et al. 2012). In the case of gyrase however, no structure with the C-gate open is available so it is difficult to conclude. It has also been suggested that the transported DNA segment itself controls the opening of the various interface for instance by “pushing open” the DNA-gate (Roca 2004, Bax, Murshudov et al. 2019).

DNA gyrase is the target for the clinically important antibiotics, the fluoroquinolones. These compounds bind the enzyme and stabilize the cleaved state, the so-called “cleavage complex”. The resulting DSBs are deleterious for the bacterial cell and are thought to be the basis for their antibacterial properties. However, *in vitro*, the cleavage complexes stabilized by fluoroquinolones are reversible, showing that the enzyme subunits do not come apart. It is therefore unclear how the reversible cleavage complexes are converted *in vivo* to irreversible DNA lesions. However, treatment of bacterial cells by fluoroquinolones clearly results in DSBs (Chen, Malik et al. 1996, Bush, Diez-Santos et al. 2020). In eukaryotic cells, pathways exist for the removal of the covalently bound topoisomerase II enzyme and exposure of the DNA lesion to regular DNA repair mechanisms (Pommier, Huang et al. 2014). In bacterial cells such pathways are not well known (but see (Huang, Michaels et al. 2021)).

Some work has also suggested that in *Escherichia coli* cleavage complexes can induce illegitimate recombination between two DNA segments (Ikeda, Moriya et al. 1981, Ikeda 1994, Ikeda, Shiraishi et al. 2004). One possible mechanism being the exchange of subunits between two cleavage complexes, followed by re-ligation. However, these experiments were conducted in a complex cellular extract and whether the observed recombination occurs through subunit exchange is not known. It has been shown that treatment with fluoroquinolones is associated with genomic rearrangements (López, Elez et al. 2007, LóPez and BláZquez 2009), potentially playing a role in their cytotoxicity, but again the exact mechanism remains unclear.

In this work we purify *E. coli* gyrase complexes with a heterodimeric GyrA interface as pioneered in the Klostermeier group (Gubaev, Weidlich et al. 2016). The complexes are purified as a dimer of GyrA and a fusion of GyrB and GyrA, encoded by different plasmids and thus allowing the introduction of targeted mutations on one side only of the complex. An active enzyme is reconstituted by the addition of free purified GyrB. We show that mutating the catalytic tyrosine on one side completely abolishes cleavage on this side of the complex. We show that the complex can exchange its subunits as evidenced by the reconstitution of double-strand cleavage activity. Subunit exchange does not occur with the heterodimeric complex alone but requires the presence of the free GyrB subunit. We show that GyrB can multimerize and pull the heterodimers into higher-order multimers. We also show that mutating isoleucine 174 in GyrA (*E. coli* numbering) abolishes DNA cleavage but not DNA binding and only lowers wrapping activity. Introducing the I174G mutation on one side of the heterodimer severely reduces cleavage activity suggesting that proper DNA bending and/or wrapping favors subunit exchange. Altogether, our data suggest that DNA binding and wrapping and the accumulation of gyrase in higher-order oligomers can favor rapid subunit exchange between two active gyrase complexes brought into proximity. We discuss

the possible mechanism and suggest that gyrase can recombine two DNA duplexes through subunit exchange.

MATERIALS AND METHODS

Expression and purification of GyrA-GyrBA heterodimer, GyrB and GyrA.

The full *E. coli* GyrA coding sequence was cloned in pACYC-Duet (from Millipore/Novagen) under the T7 promoter. A fusion of *E. coli gyrB* followed by *E. coli gyrA*, without linker was cloned into pTTQ18, under the tac promoter. A 6xHis tag is added at the N-terminus of GyrB. Both plasmids were co-transformed into *E. coli* BLR competent cells (Millipore/Novagen). Expression was initiated by the addition of 1 mM IPTG to 1 l of log-phase culture in LB and allowed to proceed for 3 h at 37° C. Cells were then pelleted and kept at -80° C until the purification procedure was performed. Expression of GyrBA is much lower than GyrA and ensure that only a low amount of GyrBA fusion homodimers is formed (Supp. Fig. 1a). For purification the cells were resuspended in 10 ml of 50 mM Tris·HCl (pH 7.5), 10% sucrose, 10 mM KCl, 1 mM EDTA, 2 mM DTT buffer to which was added 1 tablet of complete EDTA-free protease inhibitors cocktail (Roche). The cells were lysed by passage through an Avestin high pressure system at 45 psi. The lysate was cleared by centrifugation and loaded on to a 5 ml Ni^{2+} column at 0.5 ml/min in 50 mM Tris·HCl (pH 7.5), 1 mM EDTA, 2 mM DTT, 20 mM imidazole. Elution proceeded in a 30 ml gradient to 500 mM imidazole. The heterodimer fractions were collected, concentrated and loaded onto a Superose 6 column and eluted in 50 mM Tris·HCl (pH 7.5), 1 mM EDTA, 2 mM DTT. The heterodimers fractions were pooled and concentrated to around 2 mg/ml. Glycerol (to 10%) and KCl (to 100 mM) were added, and the preparation frozen in small aliquots in liquid N_2 and kept at -80° C. A monoQ step can be added before the Ni^{2+} column and this increases the purity of the preparation and lowers background cleavage. However, results are similar. The individual gyrase subunits GyrA and GyrB were prepared as described previously (Maxwell and Howells 1999).

Cleavage assays

Cleavage reactions were performed as described previously (Reece and Maxwell 1989) with some modifications. 500 ng of relaxed pBR322 plasmid is used in each 30 µL reaction containing 35 mM Tris·HCl (pH 7.5), 24 mM KCl, 4 mM $MgCl_2$, 2 mM DTT, 6.5 % (w/v) glycerol, and 0.1 mg/ml albumin. The reactions were carried out for 30 min (unless indicated otherwise) at 37°C. The amount of gyrase preparation added to each reaction is indicated for each experiment. Cleavage complexes were trapped by the addition of 7.5 µL of 1% (w/v) SDS. The cleavage products were then digested with 20 µg of proteinase K for 1 h at 37°C. The cleaved DNAs were analyzed using 1% agarose electrophoresis in the presence 0.5 µg/ml ethidium bromide. In these conditions, intact DNA plasmids migrate as a single band (topoisomers are not resolved). Gels were quantified with imageJ and the data treated and plotted with Scipy (Jones, Oliphant et al. 2001).

Supercoiling assays

Supercoiling reactions were performed as described previously (Reece and Maxwell 1989). 500 ng of relaxed pBR322 plasmid was used as a substrate in a 30 µL reaction containing 35 mM Tris·HCl (pH 7.5), 24 mM KCl, 4 mM MgCl2, 2 mM DTT, 6.5 % (w/v) glycerol, 1.8 mM spermidine, 1 mM ATP and 0.1 mg/ml albumin. The reactions were carried out for 30 min at 37°C. The amount of enzyme added varies and is indicated for each experiment. It is usually kept limiting to compare different preparation. The efficiency of supercoiling can vary depending on the assay buffer stock and GyrB preparation used. In this manuscript, assays presented in the same figure (supplementary and main) are all done with the same buffer stock and GyrB preparation.

Blue-native PAGE

Proteins (normally between 0.1 µg and 2 µg) were added, along with other relevant factors, such as ATP, DNA and or antibiotics, native-PAGE sample buffer (2.5 µL of a 4 × solution - 50 mM Bis-Tris (pH 7.2), 6 M HCl, 50 mM NaCl, 10% (w/v) glycerol, and 0.001% Ponceau S in Milli-Q® Ultrapure H_2O) and ultrapure water (to a final volume of 10 µL) to a 10 or 15 well NativePAGE™ Novex® 4 – 16% gradient Bis-Tris Gel (Life Technologies). Gels were placed in a XCell SureLock™ Mini-Cell Electrophoresis System in the cold room (~7°C). The upper buffer chamber was filled with cold 1 × Cathode buffer (50 mM Tricine, 15 mM Bis-Tris and 0.002% Coomassie G250 in Milli-Q® Ultrapure H_2O, pH 7.0) and the lower chamber filled with cold 1 × Anode buffer (50 mM Bis-Tris (pH 7.0) in Milli-Q® Ultrapure H_2O). The gels were run at 150 V, restricted to 8 mA (max 10 mA for 2 gels) for 1 h, after which the voltage was increased to 250 V, restricted to 2 mA per gel for a further 2 h. The gels were either stained with InstantBlue Coomassie (Expedeon) stain or transferred for Western Blotting. Gel pictures were taken using a Syngene G:BOX Gel Doc system.

Western blot for BN-PAGE

Polyacrylamide gels were transferred to PVDF membranes using the BioRad Trans-Blot® Turbo™ system at 20 V, 2.5 mA, for 15 min. After transfer, membranes were briefly washed with Ponceau S then rinsed with ultrapure MilliQ H_2O. The membrane was blocked in TBS-T (50 mM Tris.HCl pH 7.6, 150 mM NaCl, 0.1% Tween-20) with 5% milk solids (Marvel Dry Skimmed Milk powder) for 10 min before incubating at 4°C overnight with monoclonal antibody (either anti-GyrA-CTD – 4D3 or anti-GyrB-CTD – 9G8; a gift from Alison Howells, Inspiralis) diluted 1/1000 in TBS-T 5% milk. The membrane was then rinsed briefly with TBS-T before washing three times for 10 min each at room temperature. The membrane was then incubated at room temperature for 1 h with secondary antibody (1/5000); rabbit polyclonal antimouse-HRP conjugate (Dako). This was then washed as described above. The membrane was flooded with Pierce™ ECL Western Blotting Substrate and left for 1 min at room temperature before

covering with Clingfilm and exposed for 5 – 10 min onto Amersham Hyperfilm ECL Auto Radiography film before developing in a Konica Minolta SRX101A developer.

Mass Photometry

We performed measurements using the first generation of Refeyn instrument. The protein preparations were diluted to the optimal concentration (as determined through trial-and-error) in the cleavage reaction buffer used for cleavage assay. 10 µl of buffer was deposited on a glass slide cleaned by sonication in isopropanol. Focus was established automatically by the instrument and 1 to 2 µl of the diluted preparation was added and mixed rapidly by pipetting. A 6000-frame movie of the collisions was recorded and analyzed with the Refeyn software (AcquireMP and DiscoverMP, respectively). The contrast of the landing events on the surface (point spread functions) are analyzed and converted to a molecular mass by using a calibrant (Urease) that has well-defined molecular mass peaks (91, 272 and 545 kDa). The number of collisions is plotted against the measured molecular weight and the peaks were fitted to gaussian using DiscoverMP.

Cleavage-induced radiolabeling of heterodimeric gyrase

Relaxed pBR322 was radiolabeled using a commercial nick-translation kit and α^{32}P-dCTP. Cleavage assays were then performed as above replacing the DNA substrate with 250 ng of radiolabelled DNA. Around 10 pmole of heterodimers are used for each reaction and following SDS-trapping, no proteinase K is added. 150 mM of NaCl is added along with 10 µg of albumin and the cleavage complexes were precipitated by addition of 2 volume of absolute ethanol. The pellets were resuspended in 20 µl water and digested with micrococcal nuclease. The labelled proteins are analysed by SDS-PAGE. Following migration, the gel is dried and exposed to a phosphor screen.

Native mass spectrometry

The protein preparation was stored at −20 °C before being buffer exchanged into 200 mM ammonium acetate (pH 6.8) by multiple rounds of concentration and dilution using the Pierce™ protein concentrators (Thermo Fisher). The sample was then diluted to 2 micromolar monomer concentration immediately before the measurements. The data was collected using in-house gold-plated capillaries on a Q Exactive™ mass spectrometer in positive ion mode with a source temperature of 50 °C and a capillary voltage of 1.2 kV. For Gyrase A, in-source trapping was set to −200 V to help with the dissociation of small ion adducts and HCD voltage was set to 200 V. For BA_F.A, the voltages were set to -100 V and -100 V for in-source trapping and HCD, respectively. Ion transfer optics and voltage gradient throughout the instruments were optimized for ideal transmission. Spectra were acquired with 10 microscans to increase the signal-to-noise ratio with transient times of 64 ms, corresponding to the resolution of 17,500 at $m/z = 200$, and AGC target of 1.0×10^6. The noise threshold parameter was set to 3 and variable m/z scan ranges were used.

RESULTS

Preparation of stable GyrA-GyrBA heterodimers

Our initial aim was to study the cooperativity between the two sides of the dyad axis. Inspired by the Klostermeier group (Gubaev, Weidlich et al. 2016), we developed a procedure to express and purify heterodimers of GyrA and a GyrB-GyrA fusion construct. The fusion is N-terminally tagged with 6xHis. Co-expressing both constructs in *E. coli* yields a reasonable amount of heterodimers (around 1 mg for 1 L of culture). They are purified by a combination of Ni^{2+} affinity, ion exchange and size exclusion chromatography (see Materials and Methods). The quality of the preparations was assessed by analytical gel filtration (Supp. Fig. 1c), Blue-Native PAGE, Mass Photometry and native mass spectrometry (Fig. 2, Supp. Fig. 2 and Supp. Fig. 6a). Our heterodimer preparation showed a single-peak on a gel-filtration column, distinct from the GyrA dimer peak. An SDS-PAGE analysis of the peak showed two bands, whose sizes are consistent with GyrA and the GyrBA fusion construct (Supp. Fig. 1b). We also compared our different preparations by Blue-native PAGE. GyrA protein migrates mainly as dimers, but tetramers (slower migrating band marked "A_4 tetramer", Fig. 2, Supp. Fig. 6a) and potentially higher-order oligomers are also observed. GyrB migrates as a monomer but a ladder of bands with slower migration are also observed (Fig 2a and Supp. Fig 6a), showing the propensity of *E. coli* GyrB to multimerize. Compared to these preparations, our heterodimer preparation migrates mainly in a band intermediate between the GyrA dimer and the GyrA tetramer, again consistent with the theoretical MW of the complex. Some higher-order complexes (i.e. multimers) are also detected (slower migrating species) in the heterodimer preparation, consistent with the observation that both GyrA dimers and GyrB monomers can multimerize, presumably conferring the heterodimer the ability to multimerize.

We also used mass photometry to analyze our preparations. This technique analyzes the light scattered by molecules in solution when they hit a glass surface (Young, Hundt et al. 2018). The scattering intensity correlates with the molecular weight of the particles. The resulting histograms can be fitted to a gaussian and calibrated with a known preparation (urease here). This allows the estimation of the MW of particles in the preparation. Our GyrA preparation shows two peaks, one at around ~200 kDa, consistent with the GyrA dimer and one at around ~80-90 kDa, consistent with the GyrA monomer. This is surprising considering that the monomer is not detected by either gel filtration or Blue-native PAGE (Fig. 2, Supp. Fig. 1 and Supp. Fig 6a). It should be noted that for mass photometry the samples are diluted to an appropriate concentration to allow a limited number of collision events on the glass slide. This dilution varies depending on the sample being analyzed, presumably due to difference in the way different complexes and protein interact with the glass surface. In the case of GyrA the dilution was important and the concentration the mass photometry sample is around 25 nM. At such dilution some dissociation is expected, and we calculated a dissociation constant of 5.7 nM. This is close to the affinity seen with

antibodies for instance and suggests a strong GyrA interface. In the case of gel-filtration and blue-native PAGE the concentration is much higher as the preparation is not diluted (around 400 times higher). Assuming the accuracy of our previously estimated dissociation constant we calculate that the monomer/dimer ratio should be around 1 to 100 at this concentration, thus explaining why the monomers are not detected. In the case of our heterodimer preparation, we detect a main peak at the expected MW (286 kDa), very low monomer and no GyrA dimers. This shows that our heterodimer preparations are not contaminated with GyrA dimers. Incubating the preparation at 37°C for 30-60 min did not change the profile, showing that subunit exchange does not occur significantly during this period and that the low amount of monomer is not sufficient for solution-based exchange (see below). The heterodimer preparation is diluted before analysis but not as much as the GyrA preparation, the dilution factor was adjusted for each preparation in order to obtain analyzable data. We can't calculate a dissociation constant for this sample since GyrA and GyrBA fusion monomer are not detectable. However, assuming that the dissociation constant for the heterodimers is similar to that of the GyrA dimer, we calculate that the monomer/dimer ratio at this concentration should be just below 1 in 10. This appears generally consistent with our mass photometry profile and indicates that the concentration of monomer is very low at working concentrations of DNA gyrase (in DNA cleavage assay) and *a fortiori in vivo*. We also detect a peak consistent with a heterotetramer, which could be consistent with either a heterodimer binding a contaminating GyrB monomer (BA.A.B trimer), or more likely contaminating GyrBA fusion dimers (BA_2). The amount remains low and produces low background DNA cleavage in a cleavage assay (see below). We also detect a complex consistent with a dimer of heterodimers. It should be noted that the heterodimer preparation shows a wider range of size, and the maximum number of collisions that can be analyzed is constant. Therefore, the number of collisions assigned to a single species in the sample will be lower than for a more homogeneous sample (like GyrA, see the overlay in Fig 2D). This increases the error in the molecular weight measurement of minor species. In addition, the sensitivity for the detection of minor species is reduced in complex samples. To make sure that a potential GyrA contamination can be detected with reasonable sensitivity in the heterodimer preparation we have also measured preparations of GyrA and BA.A heterodimer mixed at different ratio. We observed that a very low amount of GyrA can be detected in the mix, along with the BA.A peak. Showing that any contamination with GyrA dimer would be extremely low, below the detection level. Moreover, the GyrA dimer is detected at a very high sensitivity with mass photometry as evidenced by the high dilution required to achieve the optimal number of collisions on the glass slide. Altogether, these data show that our heterodimer preparation is not significantly contaminated by GyrA dimer but has some contamination by either a BA_2 homodimer or a BA.A.B trimer. According to our mass photometry data, this contamination accounts for 14 % of the preparation (Fig. 2C), the majority of which is constituted by genuine heterodimers.

We have also analysed our GyrA and heterodimer preparation by native mass spectrometry. The GyrA dimer was readily detectable with the expected mass (194 kDa). The profile is entirely consistent with our mass photometry profiles and our BN-PAGE experiment, showing a GyrA monomer (97 kDa), a GyrA

tetramer (388 kDa) and even possibly a hexamer. The heterodimer preparation showed a peak at the expected size for a heterodimer (289 kDa) and a GyrA monomer peak (according to the size, 97 kDa). This is consistent with our mass photometry profiles with the exception of the BA_2 or BA.A.B contamination, which is not detectable by mass spectrometry.

Heterodimers with one catalytic tyrosine mutated can reconstitute double-strand cleavage activity.

We have tested our heterodimers in both cleavage and supercoiling assays. Free GyrB was added to the heterodimer prep to reconstitute an active enzyme. The wild-type heterodimer displayed robust double-strand cleavage activity in the presence of 20 μM ciprofloxacin and can negatively supercoil DNA (Fig. 3). We mutated the catalytic tyrosine to a phenylalanine on the GyrA side of the complex ($BA.A_F$) and the resulting enzyme displayed a severely reduced double-strand cleavage activity in the presence of ciprofloxacin and now displayed a robust single-strand cleavage activity. This is reminiscent of results obtained previously (Gubaev, Weidlich et al. 2016). This result is consistent with the formation of a cleavage complex with only one catalytic tyrosine. The supercoiling activity was drastically reduced as well, although not completely abolished, again consistent with earlier work (Gubaev, Weidlich et al. 2016). In both wild type and mutant, both the cleavage and supercoiling activity are dependent upon the addition of GyrB, as expected. When we introduced the tyrosine mutation on the GyrBA fusion side of the complex ($BA_F.A$) we observed, in addition to the expected single-strand cleavage activity, a very high level of double-strand cleavage, correlating with a restored high supercoiling activity, comparable to the wild type. Both activities were again dependent upon the addition of GyrB. This was unexpected and could be interpreted as: (1) an initial contamination of the heterodimer preparation with GyrA dimers, (2) subunit exchange between two heterodimers, or (3) an alternative nucleophile from the polypeptidic chain able to catalyze the same transesterification as the catalytic tyrosine. We ruled out a simple nuclease contamination since this double-strand cleavage is only observed in the presence of ciprofloxacin and is reversible (see below for further evidence). We also ruled out an initial GyrA contamination since our mutant heterodimer preparations did not show the presence of any GyrA dimers either by gel filtration, Blue-native PAGE or mass photometry (see above). Cleavage complexes are trapped at the phenol-aqueous interface when performing a phenol extraction of the sample. It is therefore possible to purify nucleic acids that are covalently linked to the enzyme by harvesting nucleic acids trapped at the phenol-aqueous interface (Materials and Methods). We observe that the single-strand cleaved DNA produced by the $BA.A_F$ plus GyrB is recovered from the phenol interface, as expected (Supp. Fig. 3). We also recovered a significant amount of double-strand cleaved DNA from the phenol interface, suggesting that the ability of this mutant heterodimer to reconstitute double-strand cleavage activity is also present, as in the case of $BA_F.A$ mutant, only much reduced. This double-strand cleavage activity was dependent on the addition of GyrB, which differentiates it from GyrB-independent background double-strand cleavage, due

to contaminating GyrBA fusion homodimer. Therefore, both BA_F.A and BA.A_F homodimer mutants can reconstitute double-strand cleavage activity *in vitro* in the presence of GyrB, albeit at different levels (see discussion for possible reasons for this asymmetry). Consequently, both mutants must be able to reconstitute strand-passage activity, which is consistent with both displaying GyrB-dependent supercoiling activity. The level of supercoiling activity correlates with the level of double-strand cleavage activity, further supporting this interpretation.

The reconstituted double-strand cleavage activity is not due to an alternative nucleophile

We next considered the possibility that the reconstituted double-strand cleavage is due to an alternative nucleophile that substitutes for the tyrosine on the mutated side. This nucleophile could be provided by the polypeptidic chain or even by the solvent in the form of a water molecule (like a nuclease). The catalytic tyrosine is surrounded by potential nucleophiles: an arginine on the N side and a threonine on the C side, forming the peptidic sequence RYT. We therefore mutated these residues to leucines and tested them in our heterodimer system. We tested three mutants: the BA_{RFA}.A, where the tyrosine is mutated to a phenylalanine and the threonine to an alanine, the BA_{RLL}.A, where both tyrosine and threonine are mutated to leucines, and the BA_{LLL}.A, where all three are mutated to leucines. All three mutants displayed robust reconstitution of double-strand cleavage activity. In fact, in all three mutants, the double strand cleavage was elevated at identical enzyme concentration (Supp. Fig. 4, discussed below). Therefore, if an alternative nucleophile was present, it would have to come from somewhere else along the peptidic chain. To completely exclude this possibility, we performed cleavage assays with radiolabeled DNA (Fig. 4). The subsequent treatment with micrococcal nuclease leaves a stub of radiolabeled nucleic acid covalently linked to the polypeptide that provided the nucleophile. The protein can be then resolved by SDS-PAGE and detected by exposure to a phosphor screen. In the case of the wild-type heterodimer, both the GyrBA fusion and GyrA are labelled, consistent with both sides providing tyrosine as a nucleophile (Fig. 4). Omitting Mg^{2+} from the cleavage reaction drastically reduced the signal on both sides. With the heterodimer mutants, the signal is abolished on the side where the tyrosine is mutated, showing that tyrosine is absolutely required for cleavage and that no alternative nucleophile from the polypeptidic chain can substitute for it (Fig. 4). The low amount of GyrA labelling observed in the BA.A_F mutant is probably due to a very small amount of contaminating wild-type GyrA from the endogenous (chromosomal) *gyrA* gene in the *E. coli* expression strain. There is no background labelling at all for the GyrBA fusion since the coding sequence is absent in *E. coli*. This demonstrates that there is no nucleophile from the polypeptidic chain that can substitute for tyrosine.

However, there is a possibility that the nucleophile comes from the solvent in the form of a water molecule. If this was the case, the 5′ end of the cleaved DNA would be exposed to exonuclease treatment and would not be protected by the normally covalently bonded polypeptide. We therefore performed a cleavage assay and compared the sensitivity of the cleaved products to T5 exonuclease, which requires a

5′ DNA end to degrade DNA, and Exonuclease III which requires a 3′ end. In both cases we added a DNA PCR fragment to control for nuclease activity. Both nucleases were unable to digest intact plasmidic DNA as expected but were able to digest the control DNA fragment. Exo III was able to digest the gyrase cleavage product since the covalent link is established on the 5′ end, as expected. On the other hand, the gyrase cleavage products were resistant to T5 exo digestion, showing that the 5′ end of the cleaved product is protected by a covalently linked polypeptide, even when the tyrosine is mutated (Supp. Fig. 5).

From all the experiments above, we suggest that the reconstitution of double-strand cleavage activity must come from subunit exchange between two heterodimers.

Free GyrB favors subunit exchange

In all the experiments above, GyrB was added at approximately 2-fold excess compared to the heterodimers. At this concentration, we observe GyrB-dependent double-strand cleavage with $BA.A_F$. However, the only active product of subunit exchange (GyrBA fusion homodimer) for this construct should not require GyrB for its cleavage activity. We therefore interpret this result as GyrB promoting subunit exchange, an additional activity to its classic role within a gyrase complex. We therefore tested the effect of varying GyrB concentration on the cleavage activity of the wild-type heterodimer (BA.A) compared to $BA_F.A$ (Fig. 5). In the case of the wild-type enzyme, robust double-strand cleavage activity at all GyrB concentrations was observed. Increasing the concentration of GyrB only marginally stimulated DSBs. Interestingly, robust double-strand cleavage activity was even observed at low GyrB/heterodimer ratio (less than one GyrB monomer for one heterodimer) suggesting that heterodimers alone can maintain a cleavage complex (although GyrB would still be needed for their formation, since they are not observed in the complete absence of GyrB). In the case of $BA_F.A$, adding GyrB at low concentration (GyrB/heterodimers < 1) produced almost only single-strand broken cleavage complexes, whereas GyrB added at a high concentration (GyrB/heterodimers > 1) produced the reconstitution of a robust double-strand cleavage activity. This shows that our mutant heterodimer with a single catalytic tyrosine behaves as expected at low GyrB concentration and is indeed able to form single-strand cleavage complexes and further disproves the possibility of an initial GyrA dimer contamination of our preparations. In addition, this experiment shows that the reconstitution of double-strand cleavage activity and therefore subunit exchange, is stimulated by a higher GyrB/heterodimer ratio.

DNA bending and the wrapping domain favor subunit exchange

We next tested a construct were the CTD on the GyrA side of the heterodimer is deleted, abolishing the ability to wrap DNA on this side. This construct is dubbed A_{59} (Reece and Maxwell 1991), since the truncated GyrA is down to 59 kDa. We compared $BA.A_{59}$ to $BA_F.A_{59}$ (Fig. 6a,b). The wild-type enzyme displayed a robust double-strand cleavage activity and supercoiling activity, consistent with results from

Klostermeier that show only one wrapping domain is sufficient for supercoiling activity (Stelljes, Weidlich et al. 2018). The $BA_F.A_{59}$ mutant displayed mostly single-strand cleavage activity with minimal reconstitution of double-strand cleavage activity, in striking contrast with $BA_F.A$ (at identical GyrB concentrations, and with the same GyrB preparation) (compare to Fig. 3 and 6c). We therefore conclude that the wrapping domain favors subunit exchange. The $BA_F.A_{59}$ mutant also showed reduced supercoiling activity compared to $BA.A_{59}$ but interestingly it is not abolished. This observation is puzzling since subunit exchange should not result in the reconstitution of an enzyme capable of supercoiling, since one side is missing a wrapping domain, while the other is missing a catalytic tyrosine. Similar results were obtained by (Gubaev, Weidlich et al. 2016) and were interpreted as evidence for a novel nicking/swiveling mechanism for the introduction of negative supercoiling by DNA gyrase; a mechanism that would only require a single tyrosine and a single wrapping domain. However, considering that DNA gyrase is extremely efficient in supercoiling, a very low amount of contaminating enzyme could produce detectable supercoiling activity when the main enzyme in the preparation is inactive, whereas a much higher enzyme concentration is needed to detect DNA cleavage. In our case, we surmise that our preparation is contaminated with a very low amount of $BA_F.A$ heterodimer, where the GyrA side is encoded by the endogenous *gyrA* gene from the expression strain (consistent with the low GyrA radiolabeling seen above). This GyrA would have the CTD and subunit exchange would produce enough active GyrA dimer to detect supercoiling but insufficient amount to detect DNA cleavage (see Discussion). We also compared $BA_F.A_{59}$ to $BA_{LLL}.A_{59}$ the LLL mutation favors subunit exchange in the construct with both CTD domains present and we found that it also favors reconstitution of double-strand cleavage activity when one CTD is absent. (See discussion for possible explanations, Supp Fig. 6). Subunit exchange on the $BA_{LLL}.A_{59}$ should reconstitute an A_{59} dimer, which is active for cleavage but cannot supercoil DNA. The double-strand cleavage observed with $BA_{LLL}.A_{59}$ did not correlate with an increase in supercoiling activity, compared with $BA_F.A_{59}$ (Supp. Fig. 6). This is consistent with the interpretation that the increased cleavage observed with $BA_{LLL}.A_{59}$ is due to the production of A_{59} dimer by subunit exchange. In addition, this observation also further disprove the hypothesis that this double strand cleavage is due to an alternative nucleophile in the $BA_{LLL}.A_{59}$ heterodimer since a heterodimer with double-strand cleavage activity and only one CTD (like $BA.A_{59}$) can supercoil DNA: if the $BA_{LLL}.A_{59}$ heterodimer had double-strand cleavage activity due to an alternative nucleophile, it is expected it could supercoil DNA, as it possess a CTD, unlike the A_{59} dimers.

Next, we considered the effect of DNA binding itself on subunit exchange. To do that we needed to affect DNA binding to the heterodimer, without affecting the GyrA side since DNA cleavage by GyrA dimers is our readout for subunit exchange. We therefore mutated Isoleucine 174, whose side chain “pokes” between two bases of the bound G-segment DNA and introduce a “kink” on each side. This severely bends the DNA that is being cleaved by the enzyme. It has been shown that mutating this residue abolished DNA bending, cleavage and strand passage activity in topoisomerase IV (Lee, Dong et al. 2013). When mutated to a glycine in *E. coli* gyrase, we found that the cleavage and supercoiling

activity were abolished with dimeric $GyrA_{I174G}$ in the presence of GyrB (Supp. Fig.7). DNA binding was still present however, consistent with earlier work (Lee, Dong et al. 2013). Moreover, we tested the ability of the mutant to wrap DNA by topological footprinting and found that the mutation did not abolish the wrapping, although it lowered its efficiency. This suggests that DNA gyrase can wrap DNA prior to DNA bending. We introduced the I174G mutation on the GyrBA fusion side of the heterodimer (forming the BA_G.A construct) and tested the construct for cleavage. The BA_G.A dimer had much reduced single- and double-strand cleavage activity (Fig. 6c). This result shows that abolishing DNA bending on one side is sufficient to impair cleavage on both sides. Moreover, it shows that only limited subunit exchange is happening since it would result in the formation of wild-type GyrA dimers capable of double-strand cleavage. We do detect a small amount of double-strand cleavage though and the construct can introduce negative supercoils (Fig. 6d). The BA_G.A heterodimer is not mutated for the catalytic tyrosine so it is possible that the bending induced by only one isoleucine is sufficient to produce the residual double-strand cleavage activity we observe; alternatively, subunit exchange alone could explain this residual cleavage. It should be noted that these two explanations are not mutually exclusive.

Kinetics of subunit exchange

We have also examined the kinetics of double-strand cleavage with our various constructs. With the wild-type heterodimer (BA.A) cleavage complexes appear within 1-2 minutes and reach a maximum at 5-10 minutes. With BA_F.A and BA_{LLL}.A the appearance of cleavage complexes is delayed by a few minutes and starts appearing around 5 minutes and reach a maximum at 60 minutes (Fig. 7). We show BA_{LLL}.A since the final amount of cleaved DNA is comparable to BA.A. This delay is therefore not due to a lower level of DNA cleavage (which could presumably take longer to rise above the detection level). We suggest that this delay corresponds to the time necessary for the subunit exchange to occur. Therefore, subunit exchange is rapid (around 3-5 minutes). We have also looked at subunit exchange using BN-PAGE to try and directly observe the exchange product. We have performed BN-PAGE with various gyrase species (Fig. 2 and Supp. Fig. 8a), including GyrB, GyrA, BA_F.A and A59. We have tried to mix GyrB with our heterodimer preparation to try and detect the product of exchange, without success. GyrB alone forms multimers (Fig. 2a and Supp. Fig. 8a) and its addition to BA_F.A results in a complex that does not enter the gel. We also looked at subunit exchange between a GyrA dimer and an A_{59} dimer to try and observe the formation of an A.A_{59} heterodimer. To identify the migration behavior of such a heterodimer we performed a denaturing/refolding procedure with a mix of GyrA and A_{59} preparations. Denaturing disrupt the dimers and during renaturation dimerization occurs randomly with the available monomers in solution, thereby forming A.A59 heterodimers (Supp. Fig. 8a,b). The resulting pattern on BN-PAGE is complicated by the fact that both GyrA dimers and A59 dimers can multimerize, which confer to the A.A_{59} heterodimer the ability to multimerize as well. The bands obtained on BN-PAGE after denaturation and renaturation were identified by comparison with a native molecular weight marker and their reactivity to an antibody that recognize GyrA, but not A_{59} (Supp. Fig. 8c). We assigned each band to their heterodimer/homodimer

and multimerization status (Supp. Fig. 8b). Mixing GyrA and A_{59} does not immediately results in heterodimer formation without denaturation/renaturation, showing that subunit exchange usually does not happen rapidly with GyrA alone. This is consistent with the high stability of the interface. However long incubation of the GyrA/A_{59} mix did eventually results in the formation of heterodimers (Supp. Fig. 8d). This happened without GyrB, ATP or ciprofloxacin. This slow exchange is distinct from our observed rapid reconstitution of double-strand activity which occurs in a few minutes and requires high concentration of GyrB. We conclude that the low concentration of GyrA monomer in solution (due to the stability of the interface) only allows for very slow subunit exchange between GyrA dimers and cannot account for our observation of a rapid reconstitution of double strand cleavage activity from BA_F.A. In addition, this slow exchange was not affected by GyrB (Supp. Fig. 8d) and was partially inhibited by ATP and ciprofloxacin (Supp. Fig. 8d). The rapid subunit exchange described above depends on high concentration of GyrB and is unaffected by ciprofloxacin and ATP.

DISCUSSION

In this work we have purified stable heterodimers of GyrA and a GyrBA fusion construct (Fig. 2). We have shown that mutating the catalytic tyrosine on one side of the heterodimer completely abolished cleavage on this side only (Fig. 4). We observed the reconstitution of double-strand cleavage activity from a BA_F.A and BA.A_F mutated heterodimers with mutated catalytic tyrosine on one side (Fig. 3). This activity was dependent on the addition of a high concentration of GyrB (Fig. 5). The appearance of this double-strand cleavage was delayed by a few minutes compared to the unmutated heterodimer (Fig. 7). We conclude that gyrase can rapidly (within a few minutes) exchange its subunits *in* vitro, thereby allowing the mutated heterodimer to reconstitute double-strand cleavage activity and therefore supercoiling activity (Fig. 3).
We have carefully controlled our heterodimer preparation for contaminations that could explains these results. Our heterodimer preparations do not show any contamination by GyrA dimers either on BN-PAGE, by mass photometry or native mass spectrometry (Fig. 2, Supp. Fig. 2). The low contamination by either $(BA)_2$ or BA.A.B would produce double-strand cleavage independent of GyrB addition. This background cleavage is minimal (Fig 3). Therefore, we can confidently conclude that the cleavage reconstituted with the mutated heterodimers does not arise from a contamination by GyrA dimers.
The reconstitution of double-strand cleavage correlates with the reconstitution of supercoiling activity. However, since the supercoiling reaction is extremely efficient, as opposed to cleavage, a very low amount of contaminating GyrA dimers, below detection levels, could explain the detection of low level of negative supercoiling. In the case of BA_F.A the level of supercoiling is very high, comparable to the wild-type, and cannot be explain by a sub-detection level of GyrA. However, In the case of BA.A_F, a low level of GyrA dimer, encoded by the endogenous *gyrA* gene could explain the low level of supercoiling we observe. Our GyrA preparations are usually not contaminated by endogenous GyrA. For instance, our preparation of $GyrA_{I174A}$ does not show any supercoiling activity (nor cleavage) in the presence of GyrB.

Our GyrB preparation on the other hand can be contaminated by a low amount of GyrA, undetectable with monoclonal antibodies, as evidenced by the very low level of supercoiling induced by GyrB alone at high concentration (in assays, lower concentrations are used to prevent this unwanted activity). In the case of our heterodimer preparations, both GyrA (untagged) and GyrBA fusion (his-tagged) are co-expressed in *E. coli*. Various dimeric combinations are therefore obtained in the crude extract, before purification. Since the nickel column step pulls down only the GyrBA fusion, GyrA dimers are be purified out. It is also possible that some heterodimers contain the His-tagged GyrBA fusion dimerized with a GyrA subunit encoded by the endogenous *gyrA*, even though the expression level of recombinant GyrA is very high (Supp. Fig. 1a), which should minimize their formation. Nonetheless, such complexes are expected to occur during expression and to be co-purified. We observed a low level of GyrA cleavage-dependent labeling with our $BA.A_F$ preparation, which demonstrate the existence of these complexes, which we denote $BA.A_{endogenous}$. These complexes explain the low level of supercoiling observed with the $BA_F.A_{59}$ heterodimer, which cannot reconstitute supercoiling activity by subunit exchange, since the contaminating $BA_F.A_{endogenous}$ would reconstitute a $GyrA_{endogenous}$ dimer, which is active in the presence of GyrB. It could also underlie the low level of supercoiling observed with the $BA.A_F$ heterodimer in the presence of GyrB, although such activity could also arise from the reconstituted BA fusion dimer.

The observation that heterodimeric single-sided catalytic mutant preparations (e.g., $BA.A_F$, $BA_F.A$, $BA_F.A_{59}$) still have some supercoiling activity, which we have confirmed, has led others (Gubaev, Weidlich et al. 2016) to propose a mechanism by which gyrase introduces negative supercoiling through nicking of the DNA (which requires only one catalytic tyrosine) and swivel relaxation of the DNA wrapped around the CTD domain of GyrA. We conclude that such a mechanism is most likely incorrect for several reasons. The first is a theoretical consideration. It is known that gyrase can introduce positive supercoiling by relaxing the constrained positive wrap around the CTD in the absence of ATP. Therefore, the default position of the CTD is the constraint of positive supercoils and their relaxation necessarily implies release from the CTD, which is favored by the ATPase activity of the enzyme (Basu, Schoeffler et al. 2012, Basu, Hobson et al. 2018). On average, +0.74-0.8 supercoils is constrained by wrapping around the CTD (Kampranis, Bates et al. 1999, Basu, Schoeffler et al. 2012). The relaxation of a single positive loop (with a ~+1 contribution to the ΔLk) should therefore introduces negative supercoiling by steps of 1. Only the conversion of a positive loop (+1) to a negative (-1) by strand passage can introduce supercoiling by steps of 2. Since a gyrase complex has two CTDs, it could be assumed that the simultaneous relaxation of the two loops could introduce supercoiling by step of two, however, Klostermeier and co-workers have proved that only one CTD is needed for introducing supercoils by steps of two (Stelljes, Weidlich et al. 2018). Therefore, for the model to stand, it must be assumed that, in addition to the (+1) supercoils stabilized by the writhe of the loop, another +1 must be stabilized in the twist of the double helix within this short loop. We find this to be unlikely considering recent cryo-EM structures of gyrase with DNA (Vanden Broeck, Lotz et al. 2019). However, a CTD-wrapped state with +1.7 supercoils has been detected in the absence of ATP (Basu, Schoeffler et al. 2012). It is therefore conceivable that that the relaxation of DNA

wrapped in this state could lead to the introduction of supercoiling by step of 2 *via* swiveling. This state is much less abundant than the +1 state however and the efficiency of the swiveling mechanism would be very low. For an efficient mechanism involving relaxation by swiveling of this +1.7 state one would have to assume that ATP favors its formation, in addition to promoting the release of the DNA loop. These two activities contradict each other. In addition, the addition of nucleotides either did not favor the +1.7 state or did not change its abundance (Basu, Hobson et al. 2018). Finally, this state could represent twin-wrapping around the 2 CTDs, and only one CTD is sufficient for supercoiling, as stated above. In conclusion, introduction of negative supercoiling by swiveling-mediated relaxation of the wrapped DNA loop would have to occur by steps of 1, or be extremely inefficient when they occur by step of two.

On top of the above consideration, our and others' (Gubaev, Weidlich et al. 2016) results can be explained by subunit exchange. Even in the case of the $BA_F.A_{59}$, a low level of heterodimer with endogenous GyrA could produce some active GyrA dimers by subunit exchange. In any case, mutating one catalytic tyrosine results in a drastic diminution of supercoiling activity, showing that most of the activity is based on strand passage through a double-strand break. In a configuration where the reconstitution of double-strand cleavage activity is important (such as $BA_F.A$), it correlates with a robust supercoiling activity, further supporting that supercoiling activity is based on the ability to double-strand cleave DNA. These results argue strongly against swiveling since the later only require a single-strand break, and therefore should be unaffected by mutating one catalytic tyrosine.

The reasons for the asymmetry between $BA_F.A$ and $BA.A_F$ are unclear so far. With the $BA_F.A$ heterodimer subunit exchange produces an active GyrA dimer and an inactive $(BA_F)_2$ dimer. In the case of $BA.A_F$, subunit exchange reconstitutes an active $(BA)_2$ dimer and an inactive $GyrA_F$ dimer. Therefore, the difference in the level of cleavage and supercoiling activity reconstituted could stem from a difference in activity between the GyrA dimer (with free GyrB) and the $(BA)_2$ dimer. We have directly tested this and compared both cleavage and supercoiling activity between GyrA dimer ("wild type"), $(BA)_2$ dimer and BA.A heterodimer (Supp. Fig. 9). We found that the activity of $(BA)_2$ is reduced by a factor 100. Interestingly, the heterodimer has a level activity intermediate between the GyrA dimer and the (BA)2 dimer. This is true for both cleavage and supercoiling. These results explain the asymmetry between $BA_F.A$ and $BA.A_F$ since the subunit exchange with the former produces a more active complex by subunit exchange compared to the later. These results also show that fusing GyrB to GyrA limits both cleavage and supercoiling activity. We did not add a linker to our fusion and therefore the position of GyrB with respect to GyrA and DNA is expected to be more constrained than with free GyrB. It has been reported that the GyrB dimer is leaning to one side with respect to the dyad axis in the gyrase-DNA complex (Vanden Broeck, Lotz et al. 2019). Therefore, in this complex, the position of each GyrB subunit with regard to GyrA is different and this flexibility of GyrB in the gyrase complex might be important for its activity. We speculate that with a GyrB fused to GyrA limits the leaning ability of the GyrB dimer and therefore reduces both the supercoiling activity and the ability to form cleavage complexes.

This leads us to discuss the exact mechanism of subunit exchange. It is *a priori* a surprising result considering the stability of the gyrase dyad interface and its importance in ensuring genome stability. However, during strand passage all three interfaces must be broken and the opening of the interfaces necessarily implies the possibility of exchange between two complexes prior to their reformation. The integrity of the complex is ensured through sequential opening and closing of the three interfaces. This sequential opening and closing allows the transported DNA to go through the whole complex without it coming apart. Similarly, subunit exchange could also occur sequentially, one interface after the other, allowing the exchange to occur without the complex coming apart. This model would only require gyrase complexes being able to come together and interact in an appropriate configuration and we indeed observe that both GyrA dimers and GyrB monomers can multimerize, each on their own in solution, supporting this hypothesis. In fact, our results only show that the DNA-cleaving interface is exchanged; it is possible that this is not followed by the exchange of the C-gate interface, producing a sort of helical super-complex where one interface interacts with a different subunit compared to the other interface. Structural evidence exists for such a complex. In earlier work (Rudolph and Klostermeier 2013) a GyrA structure with the DNA gate opened was obtained. The DNA gate interacts with the next GyrA subunit forming a helical oligomer of GyrA within the crystal. We suggest that this structure could underly subunit exchange in our system, with the C-gate interface remaining closed, while the DNA gate interface opens and reforms with the neighboring complex. It is even possible that such a super-complex would retain negative supercoiling activity. The opening of the DNA gate does not occur by the pulling apart of the GyrA WHD domains but rather by a sliding of the two GyrA domains against one another along an axis close to being perpendicular to a plane formed by the dyad axis and the DNA axis (Wendorff, Schmidt et al. 2012, Chen, Huang et al. 2018, Germe, Voros et al. 2018). Therefore, the freed DNA-gate interface could be available to dimerize with a neighboring interface similarly freed by the opening of the DNA gate. The only requirement being that the neighboring complex is positioned parallel to the other one, in such a way that the simultaneous opening of the DNA gates results in the meeting of the two DNA gate interfaces between the complexes. We dub this process “interface swapping” (Fig. 8).

We have tried and failed to directly observe subunit exchange by mass photometry. We tried to observe the reconstitution of a GyrA dimer from a heterodimer. However, this experiment is complicated because of several factors. The first is the necessity of a high concentration of GyrB. This will mask any GyrA monomer that might be produced and also will bind any GyrA dimer that is produced reconstituting a trimer (with a MW equivalent to the heterodimer) or a tetramer (with a MW equivalent to GyrB bound to a heterodimer) that are indistinguishable from the original complex. We have not observed a significant change of the mass photometry profile of a mixture of GyrB + BA.A heterodimer over time. In addition, our data suggest that proper DNA binding and bending is necessary for subunit exchange. Adding a long piece of DNA only scrambles the mass photometry profile as the complexes binds to it to form high MW particles. We have tried to add a short, purified DNA fragment (170 bp) which gives a nice peak on its own in mass photometry but again failed to see a difference. It could be that longer DNA is needed to

allow the wrapping of several CTDs along the DNA and position the complexes for subunit exchange (see below). It is also possible that only the DNA-gate interfaces are exchanged and therefore no GyrA dimers are ever produced, only higher MW oligomers that are difficult to detect. Indeed, interface swapping does not necessarily result in the coming apart and complete separation of the complex (see below).

We have shown that efficient subunit exchange requires the CTD or wrapping domain of GyrA. Subunit exchange is quick in our system and removing the CTD produced much less double-strand cleavage within the 30 minutes timeframe of our experiment. We suggest that the wrapping of the DNA is necessary for the positioning of two or several gyrase complexes in such way that interface exchange by the mechanism proposed above is favored. It is also possible that the CTD favor the opening of the DNA-gate interface, an idea supported by the observation that full length gyrase has ATP-independent strand passage activity but not the A_{59} dimer + GyrB. It should be noted that subunit exchange can still occur with GyrA and GyrA59 on their own but in a much longer time frame (Supp. Fig. 6). We suggest that this slow subunit exchange occurs *via* free GyrA monomers, which we have shown to exist by mass photometry. Since the GyrA interface is strong, the concentration of monomer is very low and therefore exchange by this mechanism is bound to be very slow. The rapid subunit exchange that we observe therefore likely occurs *via* a different mechanism and we suggest that it occurs by interface swapping within multimers of gyrase complexes.

We also showed that mutating isoleucine 174 drastically diminished the amount of subunit exchange. This could be interpreted in various ways. First, proper DNA bending is necessary for DNA cleavage (Dong and Berger 2007, Lee, Dong et al. 2013), and X-ray structures have shown that DNA binding and bending correlate with a slight opening of the DNA gate (Wendorff, Schmidt et al. 2012, Germe, Voros et al. 2018). Therefore, it could be that the binding of the DNA loosens the DNA gate interface and favors its opening. The second interpretation is that, although the isoleucine mutant can still bind and wrap DNA, the wrapping efficiency is reduced and therefore indirectly affects subunit exchange since the CTD is important for subunit exchange.

We also observed that mutating the two residues neighboring the catalytic tyrosine favored subunit exchange. The mutation converts polar side chains to aliphatic ones and likely affects interface interaction. Indeed, the catalytic tyrosine and its neighboring residues are in proximity to the TOPRIM domain in the gyrase apo structure (Bax, Murshudov et al. 2019). Upon binding DNA, the distance between them increases and DNA cleavage is accompanied by the full disengagement of the catalytic tyrosine from the TOPRIM domain. The opening of the DNA gate fully separates the catalytic loop, which contains the catalytic tyrosine, from the TOPRIM domain by a sliding motion. Therefore, mutations disfavoring interaction between the catalytic loop and the TOPRIM domain are likely to favor DNA gate opening and therefore subunit exchange.

Subunit exchange has been proposed as the mechanism behind DNA gyrase-mediated illegitimate recombination (Ikeda, Shiraishi et al. 2004). Gyrase was shown to be involved in the transfer of an antibiotic resistance cassette from a plasmid to lambda DNA in a packaging reaction, in the

presence of a quinolone (Ikeda, Moriya et al. 1981, Ikeda, Aoki et al. 1982).This result was independent of any homologous recombination pathway in either the phage or bacterium (Ikeda, Moriya et al. 1981, Ikeda, Aoki et al. 1982). The authors suggested that gyrase mediated recombination in one of two ways: either 1) by dissolution of the gyrase complex into heterodimers (GyrA:GyrB) that still had the DNA bound in the phosphotyrosyl bond, which could reassociate with another GyrA:GyrB heterodimer in a similar situation, allowing for recombination, or 2) by the formation of higher order oligomers ($GyrA_4GyrB_4$) and interface swapping, which upon dissolution of the higher-order complex could result in subunit exchange and recombination (Ikeda 1994, Ikeda, Shiraishi et al. 2004). We suggest the former may be the cause of slower subunit exchange observed in the formation of GyrA and GyrA59 heterodimers over several days (Suppl. Fig. 6). This slow subunit exchange is inhibited by DNA and ciprofloxacin in contrast with the rapid subunit exchange observed with heterodimers. Therefore, the two are mechanistically distinct. Indeed, solution-based slow subunit exchange requires the complete separation of the complex for the formation of free monomers but does not require the formation of higher-order oligomers. In contrast, rapid subunit exchange by interface swapping does not require the complete separation of the complex but does involve the formation of higher-order oligomers. It therefore makes sense that one, and not the other would be inhibited by DNA and ciprofloxacin. Ciprofloxacin-induced cleavage complexes do not come apart in solution, which is consistent with ciprofloxacin inhibiting the formation of free monomers. Ciprofloxacin does not prevent rapid interface swapping and it has been shown that it does not prevents DNA-gate opening (Chan, Germe et al. 2017). We surmise that illegitimate recombination occurs within higher-order oligomer formation followed by interface swapping (the DNA gate specifically). This is consistent with the timescale of illegitimate recombination and explains how two DNA duplexes are brought together for recombination by two gyrase complexes.

Considering the ubiquity and abundance of gyrase in bacterial cells, the rapid interface swapping mechanism is expected to occur *in vivo* where DNA is present and gyrase highly concentrated. If interfaces are swapped when gyrase is covalently bound to cleaved DNA on both sides, followed by re-ligation with the swapped DNA-gate, this would result in illegitimate recombination. The way the two gyrase complexes interact would bring together two DNA duplexes for recombination. The presence of fluoroquinolones, by extending the lifespan of the cleaved state, would make this process much more likely. We have observed that a high gyrase/DNA ratio in the presence of ciprofloxacin produces cleavage complexes ~200 bp apart (Supp. Fig. 10). Considering that gyrase can interact with ~150 bp of DNA through DNA wrapping, it suggests that the DNA exiting a gyrase complex is immediately engaged in another neighboring gyrase-DNA complex. We conclude that cleavage complexes can closely interact on DNA, thereby opening the possibility of micro-deletions or -inversions by interface swapping of the cleavage complexes, followed by re-ligation, which can happen within a cleavage complex if the drug is washed out especially. Longer-range genomic rearrangements are also conceivable depending on the organization of gyrase clusters in the bacterial cell. This interface swapping mechanism could therefore

have profound consequences for antibiotics treatment of infection and more generally the evolution of bacteria.

ACKNOWLEDGMENTS

We thank James Berger for critical reading of the manuscript. This work was supported by a Wellcome Trust Investigator Award (110072/Z/15/Z) and a Biotechnology and Biosciences Research Council (UK) Institute Strategic Programme Grant (BB/P012523/1),

FIGURES LEGENDS

Figure 1. **a.** Side view of *S. aureus* DNA gyrase core fusion structure (6FQV) with bound DNA (green). The GyrB segment is in purple (only the TOPRIM domain here) and the GyrA in blue. The C2 symmetry mate is rendered in gray. The inset shows the location of isoleucine 174 in red (*E. coli* numbering) which is inserted between base +8 and +9 (from scissile phosphate) and introduces a kink in the duplex. **b.** Top view of the same structure. The inset shows in light brown the catalytic tyrosine sandwiched between an arginine and a threonine and forming the triad RYT. **c.** Cartoon rendering of the DNA gyrase heterotetramer. GyrB is in purple and GyrA in blue. The segment in solid colors denote the part of the enzyme included in the *S. aureus* core fusion structure. Various domains are indicated, and the dashed line circles indicate the three interfaces that the transported DNA segment go through during strand passage. **d.** Schematic of DNA gyrase peptidic sequences, color coded as above. The core fusion construct used in structural studies is indicated.

Figure 2. Analysis of GyrA, GyrB and heterodimers preparations. **a.** Blue-Native PAGE of our GyrB, GyrA and wild-type heterodimer preparation. The bands constituted by GyrB monomers, GyrA dimers and heterodimers are indicated and were visualized by silver staining. The migration pattern was ascertained by comparison to a native marker and is consistent with mass photometry profiles below. **b.** Mass Photometry profile of the GyrA preparation. The histogram shows the counts of collisions events plotted against the scattering intensity, which is proportional to the MW and is calibrated against urease; the abscissa shows the molecular mass in kDa. The instrument fits the observed peaks to gaussian curves (continuous black lines) and the mean (MW) and deviation (σ) of the fitted curves are indicated on top of the peak, alongside the total count for the peak and the percentage of counts assigned to the peak with respect to the total number of fitted events. **b.** Mass Photometry profile of our wild-type heterodimer preparation, as above. Note that the lower the peak count, the higher the deviation. We detect a main

peak at approximately the expected size for a heterodimer. **c.** Superimposition of the two profiles (GyrA dimer in blue and heterodimer in orange) showing the difference in mass between the heterodimer and the GyrA dimer. The two profiles were collected the same day, in the same buffer and with the same calibration.

Figure 3. Reconstitution of double-strand cleavage activity in the presence of free GyrB. Both cleavage (top) and supercoiling (bottom) assays were performed were performed with BA.A, BA.A_F and BA_F.A as indicated. For cleavage assay 5, 2.5 and 1.25 pmole of heterodimers (three lanes, from left to right for each heterodimer version, the triangle shows increasing dosage of heterodimers) were used. 8 pmole of GyrB were added to reconstitute the activity (top left panel). Omitting GyrB showed only background cleavage (top center panel). GyrB alone (top right panel) showed almost undetectable cleavage activity. For supercoiling assays the dose of each subunit was reduced, so as to keep the activity limiting in the assay. 4 pmole of GyrB was added to 1.25, 0.625 and 0.312 pmole of heterodimer, the triangle showing increasing dose of the heterodimer.

Figure 4. a. Schematic of the radiolabeling of the catalytic tyrosine. The peptide RYT is shown in black, and a cleavage reaction results in a covalent bond between the catalytic tyrosine and a radiolabeled DNA (in red with asterisk). Subsequent digestion with micrococcal nuclease digests most of the DNA and leaves a stub of radiolabeled nucleic acid covalently bound to the catalytic tyrosine. **b.** The resulting labelled gyrase polypeptide can be analyzed by SDS-PAGE and detected by exposure to a phosphor screen. The cleavage reactions contained 8 pmole of GyrB and 5 pmole of heterodimer. From left to right: wild-type heterodimer with Mg^{2+}, without Mg^{2+}, BA_F.A (1), BA.A_F (2) and BA_{LLL}.A. The upper band is the fusion polypeptide, the lower band is the GyrA polypeptide. The smear at the bottom is the bulk of the digested radiolabeled DNA.

Figure 5. Effect of GyrB dose on subunit exchange. 5 pmole of heterodimers (BA.A and BA_F.A as indicated) were incubated with increasing amount of GyrB (triangle) in a cleavage assay. From the highest to the lowest dose: 16, 8, 4, 2, 1 and 0.5 pmole were used. At lower GyrB/heterodimer ratio, single-strand cleavage is predominant with BA_F.A whereas BA.A still displays robust double-strand cleavage activity. Single-strand cleavage activity does go up marginally with the wild-type protein at the lower GyrB dose, suggesting missing GyrB on one side can lead to the formation of single-strand cleavage complexes. However, even at very low GyrB/heterodimer ratio, the majority of cleavage complexes are double-stranded.

Figure 6. Effect of DNA wrapping and DNA bending defective mutants on subunit exchange. **a.** 5, 2.5 and 1.25 pmole (triangle indicate increasing dose) of BA.A_{59} and BA_F.A_{59} (as indicated) were incubated in a

cleavage assay with 8 pmole of GyrB. **b.** 2.5, 1.25 and 0.625 pmole (triangle indicate increasing dose) of BA.A_{59} and BA_F.A_{59} (as indicated) were incubated in a supercoiling assay in the presence of 4 pmole of GyrB **c.** 5, 2.5 and 1.25 pmole (triangle indicate increasing dose) of BA.A, BA_FA and BA_G.A were incubated in a cleavage assay in the presence of 8 pmole of GyrB. **d.** 2.5, 1.25 and 0.625 pmole (triangle indicate increasing dose) of BA.A_{59} and BA_F.A_{59} (as indicated) were incubated in a supercoiling assay in the presence of 4 pmole of GyrB. Omitting GyrB from all these assays abolished either the supercoiling or cleavage respectively. The exception being BA.A_{59}, which shows a small amount of double-strand cleavage in the absence of GyrB (Supp Fig. 6b)

Figure 7. Kinetics of subunit exchange. **a.** 5 pmole of either BA.A (blue) or BA_{LLL}.A (orange) were incubated with 8 pmole of GyrB in a cleavage assay for the indicated time**.** BA_{LLL}.A + GyrB reaches level of cleavage comparable to BA.A (albeit much later, around 60 minutes, not shown). **b.** Quantification of the gels shown in **a.** the proportion of linear of the total amount of material in each lane is plotted against time. The proportion of linear is normalized as the fraction of the total amount of linear reached at 60 minutes, minus background cleavage (very low in that instance) observed at the 0 time point.

Figure 8. Proposed model for interface swapping. **a.** Cartoon schematic of two gyrase complexes in close proximity, viewed from the side. Only the core complex is shown. **b.** 90° rotation view. The gyrase “super-complex” is viewed from the top. **c.** The opening of each DNA-gate interface occurs by a sliding movement (black arrows), allowing reformation of a hybrid interface, in the center of the super-complex. The DNA is not represented.

REFERENCES

Basu, A., M. Hobson, P. Lebel, L. E. Fernandes, E. M. Tretter, J. M. Berger and Z. Bryant (2018). "Dynamic coupling between conformations and nucleotide states in DNA gyrase." Nature Chemical Biology **14**(6): 565-574.

Basu, A., A. J. Schoeffler, J. M. Berger and Z. Bryant (2012). "ATP binding controls distinct structural transitions of Escherichia coli DNA gyrase in complex with DNA." Nature Structural & Molecular Biology **19**(5): 538-546.

Bates, A. D. and A. Maxwell (2007). "Energy coupling in type II topoisomerases: why do they hydrolyze ATP?" Biochemistry. **46**(27): 7929-7941. doi: 7910.1021/bi700789g. Epub 702007 Jun 700720.

Bax, B. D., G. Murshudov, A. Maxwell and T. Germe (2019). "DNA Topoisomerase Inhibitors: Trapping a DNA-Cleaving Machine in Motion." J Mol Biol **431**(18): 3427-3449.

Bush, N. G., I. Diez-Santos, L. R. Abbott and A. Maxwell (2020). "Quinolones: Mechanism, Lethality and Their Contributions to Antibiotic Resistance." Molecules **25**(23).

Bush, N. G., K. Evans-Roberts and A. Maxwell (2015). "DNA Topoisomerases." EcoSal Plus **6**(2).
Chan, P. F., T. Germe, B. D. Bax, J. Huang, R. K. Thalji, E. Bacque, A. Checchia, D. Chen, H. Cui, X. Ding, K. Ingraham, L. McCloskey, K. Raha, V. Srikannathasan, A. Maxwell and R. A. Stavenger (2017). "Thiophene antibacterials that allosterically stabilize DNA-cleavage complexes with DNA gyrase." Proc Natl Acad Sci U S A **114**(22): E4492-E4500.
Chen, C.-R., M. Malik, M. Snyder and K. Drlica (1996). "DNA Gyrase and Topoisomerase IV on the Bacterial Chromosome: Quinolone-induced DNA Cleavage." Journal of Molecular Biology **258**(4): 627-637.
Chen, S.-F., N.-L. Huang, J.-H. Lin, C.-C. Wu, Y.-R. Wang, Y.-J. Yu, M. K. Gilson and N.-L. Chan (2018). "Structural insights into the gating of DNA passage by the topoisomerase II DNA-gate." Nature Communications **9**(1).
Costenaro, L., J. G. Grossmann, C. Ebel and A. Maxwell (2007). "Modular Structure of the Full-Length DNA Gyrase B Subunit Revealed by Small-Angle X-Ray Scattering." Structure **15**(3): 329-339.
Dong, K. C. and J. M. Berger (2007). "Structural basis for gate-DNA recognition and bending by type IIA topoisomerases." Nature **450**(7173): 1201-1205.
Gellert, M., K. Mizuuchi, M. H. O'Dea, T. Itoh and J.-I. Tomizawa (1977). "Nalidixic acid resistance: A second genetic character involved in DNA gyrase activity." Proceedings of the National Academy of Sciences **74**(11): 4772-4776.
Germe, T., J. Voros, F. Jeannot, T. Taillier, R. A. Stavenger, E. Bacque, A. Maxwell and B. D. Bax (2018). "A new class of antibacterials, the imidazopyrazinones, reveal structural transitions involved in DNA gyrase poisoning and mechanisms of resistance." Nucleic Acids Res.
Gubaev, A., D. Weidlich and D. Klostermeier (2016). "DNA gyrase with a single catalytic tyrosine can catalyze DNA supercoiling by a nicking-closing mechanism." Nucleic Acids Res **44**(21): 10354-10366.
Huang, S.-Y. N., S. A. Michaels, B. B. Mitchell, N. Majdalani, A. Vanden Broeck, A. Canela, Y.-C. Tse-Dinh, V. Lamour and Y. Pommier (2021). "Exonuclease VII repairs quinolone-induced damage by resolving DNA gyrase cleavage complexes." Science Advances **7**(10).
Ikeda, H. (1994). "DNA topoisomerase-mediated illegitimate recombination." Adv Pharmacol **29a**: 147-165.
Ikeda, H., K. Aoki and A. Naito (1982). "Illegitimate recombination mediated in vitro by DNA gyrase of Escherichia coli: structure of recombinant DNA molecules." Proc Natl Acad Sci U S A **79**(12): 3724-3728.
Ikeda, H., K. Moriya and T. Matsumoto (1981). "In vitro study of illegitimate recombination: involvement of DNA gyrase." Cold Spring Harb Symp Quant Biol **45 Pt 1**: 399-408.
Ikeda, H., K. Shiraishi and Y. Ogata (2004). "Illegitimate recombination mediated by double-strand break and end-joining in Escherichia coli." Adv Biophys **38**(Complete): 3-20.
Jones, E., T. Oliphant and P. Peterson (2001). SciPy: Open Source Scientific Tools for Python.
Kampranis, S. C., A. D. Bates and A. Maxwell (1999). "A model for the mechanism of strand passage by DNA gyrase." Proceedings of the National Academy of Sciences **96**(15): 8414-8419.
Lee, I., K. C. Dong and J. M. Berger (2013). "The role of DNA bending in type IIA topoisomerase function." Nucleic Acids Res **41**(10): 5444-5456.
Lee, I., K. C. Dong and J. M. Berger (2013). "The role of DNA bending in type IIA topoisomerase function." Nucleic Acids Research **41**(10): 5444-5456.

LóPez, E. and J. S. BláZquez (2009). "Effect of Subinhibitory Concentrations of Antibiotics on Intrachromosomal Homologous Recombination in Escherichia coli." Antimicrobial Agents and Chemotherapy **53**(8): 3411-3415.
López, E., M. Elez, I. Matic and J. Blázquez (2007). "Antibiotic-mediated recombination: ciprofloxacin stimulates SOS-independent recombination of divergent sequences in Escherichia coli." Molecular Microbiology **64**(1): 83-93.
Maxwell, A. and A. J. Howells (1999). "Overexpression and purification of bacterial DNA gyrase." Methods Mol Biol **94**: 135-144.
Pommier, Y., S.-Y. N. Huang, R. Gao, B. B. Das, J. Murai and C. Marchand (2014). "Tyrosyl-DNA-phosphodiesterases (TDP1 and TDP2)." DNA Repair **19**: 114-129.
Reece, R. J. and A. Maxwell (1989). "Tryptic fragments of the Escherichia coli DNA gyrase A protein." J Biol Chem **264**(33): 19648-19653.
Reece, R. J. and A. Maxwell (1991). "Probing the limits of the DNA breakage-reunion domain of the Escherichia coli DNA gyrase A protein." J Biol Chem **266**(6): 3540-3546.
Roca, J. (2004). "The path of the DNA along the dimer interface of topoisomerase II." J Biol Chem **279**(24): 25783-25788.
Rudolph, M. G. and D. Klostermeier (2013). "Mapping the spectrum of conformational states of the DNA- and C-gates in Bacillus subtilis gyrase." J Mol Biol **425**(15): 2632-2640.
Stelljes, J. T., D. Weidlich, A. Gubaev and D. Klostermeier (2018). "Gyrase containing a single C-terminal domain catalyzes negative supercoiling of DNA by decreasing the linking number in steps of two." Nucleic Acids Res.
Sugino, A., C. L. Peebles, K. N. Kreuzer and N. R. Cozzarelli (1977). "Mechanism of action of nalidixic acid: Purification of Escherichia coli nalA gene product and its relationship to DNA gyrase and a novel nicking-closing enzyme." Proceedings of the National Academy of Sciences **74**(11): 4767-4771.
Vanden Broeck, A., C. Lotz, J. Ortiz and V. Lamour (2019). "Cryo-EM structure of the complete E. coli DNA gyrase nucleoprotein complex." Nature Communications **10**(1).
Vos, S. M., E. M. Tretter, B. H. Schmidt and J. M. Berger (2011). "All tangled up: how cells direct, manage and exploit topoisomerase function." Nature Reviews Molecular Cell Biology **12**(12): 827-841.
Wendorff, T. J., B. H. Schmidt, P. Heslop, C. A. Austin and J. M. Berger (2012). "The structure of DNA-bound human topoisomerase II alpha: conformational mechanisms for coordinating inter-subunit interactions with DNA cleavage." J Mol Biol. **424**(3-4): 109-124. doi: 110.1016/j.jmb.2012.1007.1014. Epub 2012 Jul 1025.
Young, G., N. Hundt, D. Cole, A. Fineberg, J. Andrecka, A. Tyler, A. Olerinyova, A. Ansari, E. G. Marklund, M. P. Collier, S. A. Chandler, O. Tkachenko, J. Allen, M. Crispin, N. Billington, Y. Takagi, J. R. Sellers, C. Eichmann, P. Selenko, L. Frey, R. Riek, M. R. Galpin, W. B. Struwe, J. L. P. Benesch and P. Kukura (2018). "Quantitative mass imaging of single biological macromolecules." Science **360**(6387): 423-427.

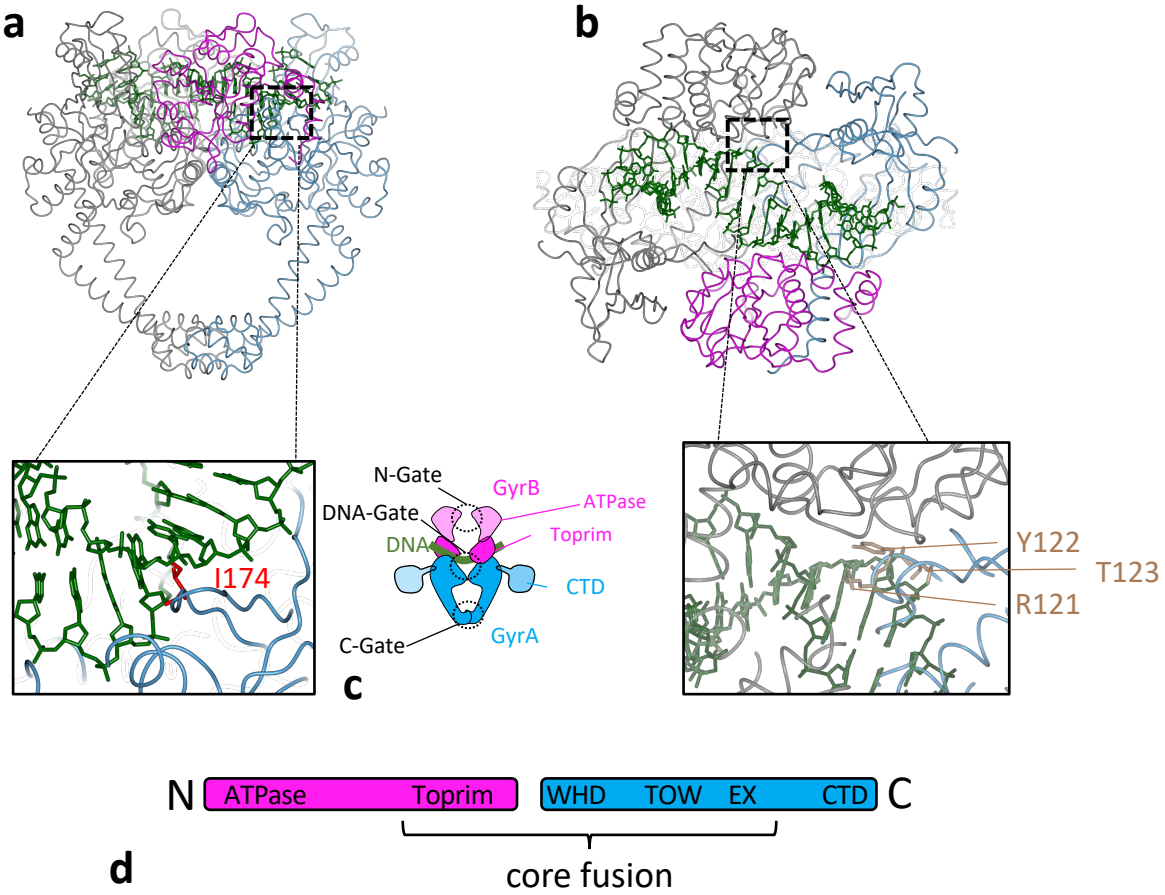
a
b
I174
N-Gate
GyrB
ATPase
DNA-Gate
Toprim
DNA
CTD
C-Gate
GyrA
c
Y122
T123
R121
N
ATPase
Toprim
WHD
TOW
EX
CTD
C
core fusion
d

Figure 1

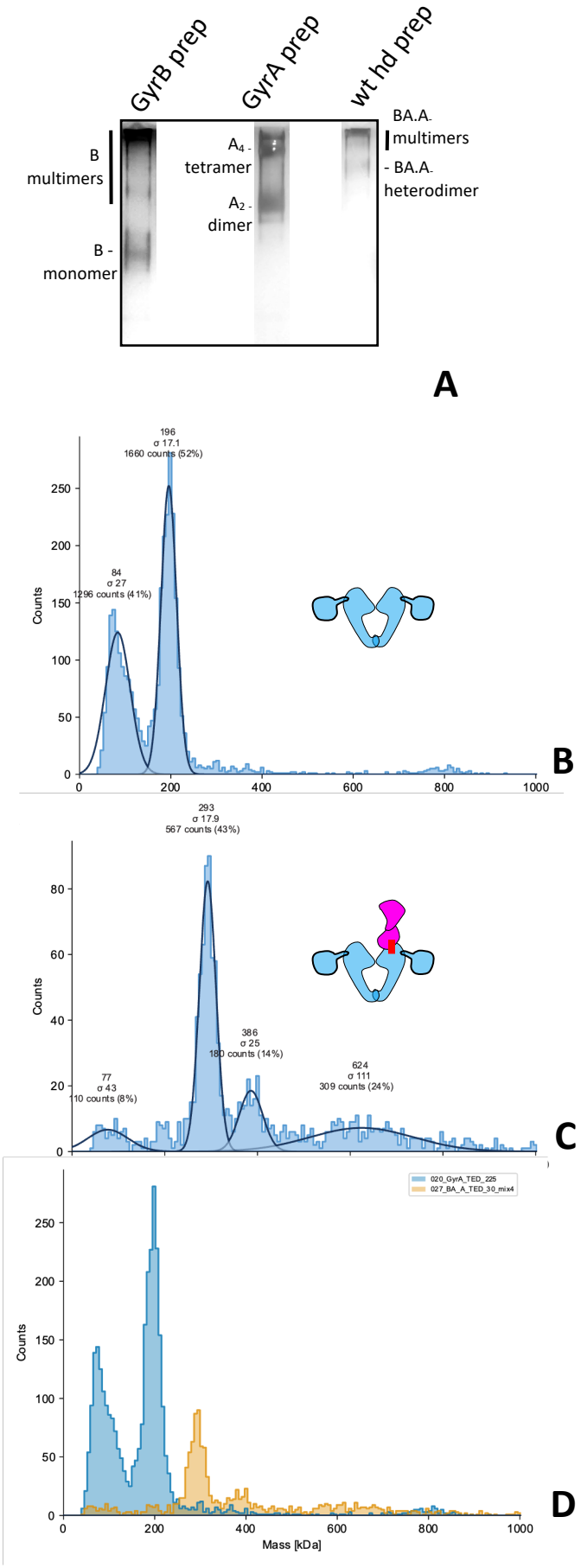
GyrB prep
GyrA prep
wt hd prep
B multimers
B - monomer
A4 - tetramer
A2 - dimer
BA.A. multimers
- BA.A. heterodimer
A
196
σ 17.1
1660 counts (52%)
84
σ 27
1296 counts (41%)
Counts
B
293
σ 17.9
567 counts (43%)
386
σ 25
180 counts (14%)
77
σ 43
110 counts (8%)
624
σ 111
309 counts (24%)
C
020_GyrA_TED_225
027_BA_A_TED_30_mix4
Mass [kDa]
D

Figure 2

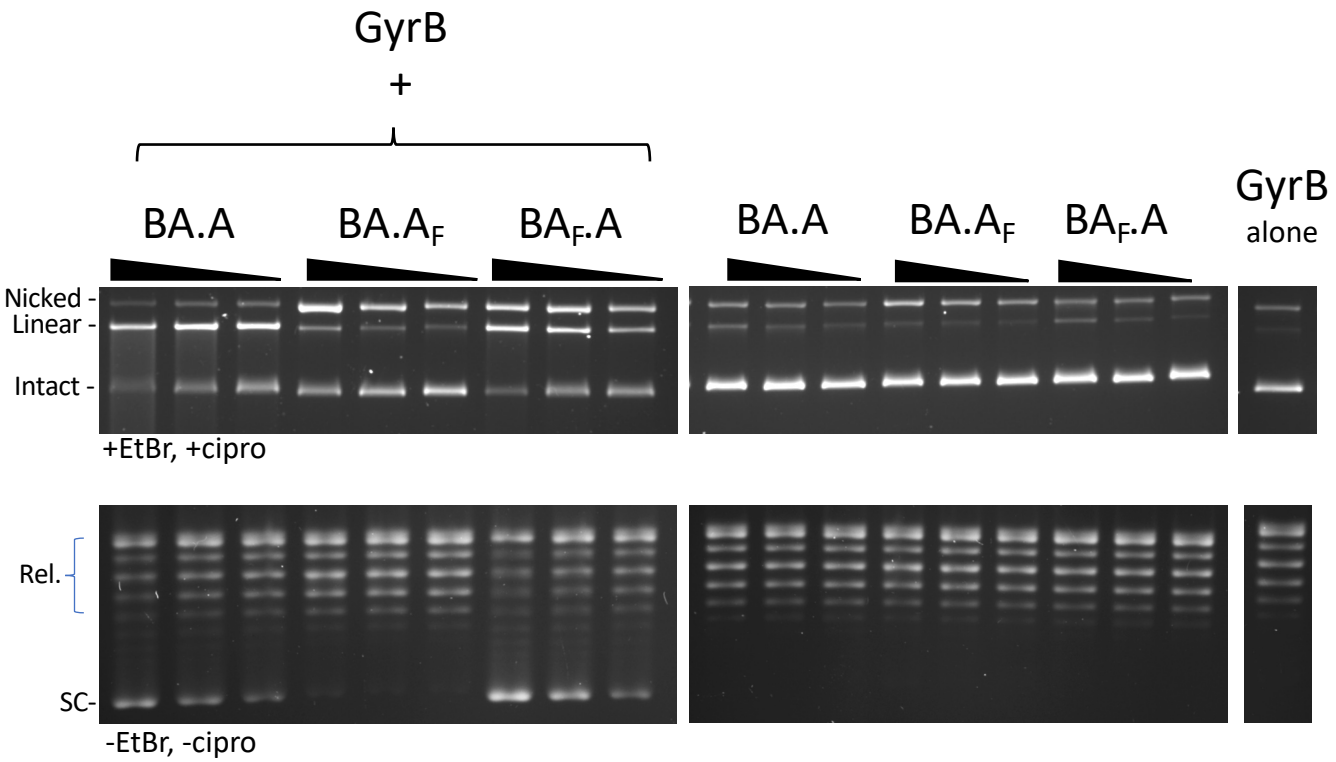
GyrB
+
BA.A
BA.A$_F$
BA$_F$.A
BA.A
BA.A$_F$
BA$_F$.A
GyrB
alone
Nicked -
Linear -
Intact -
+EtBr, +cipro
Rel.
SC-
-EtBr, -cipro

Figure 3

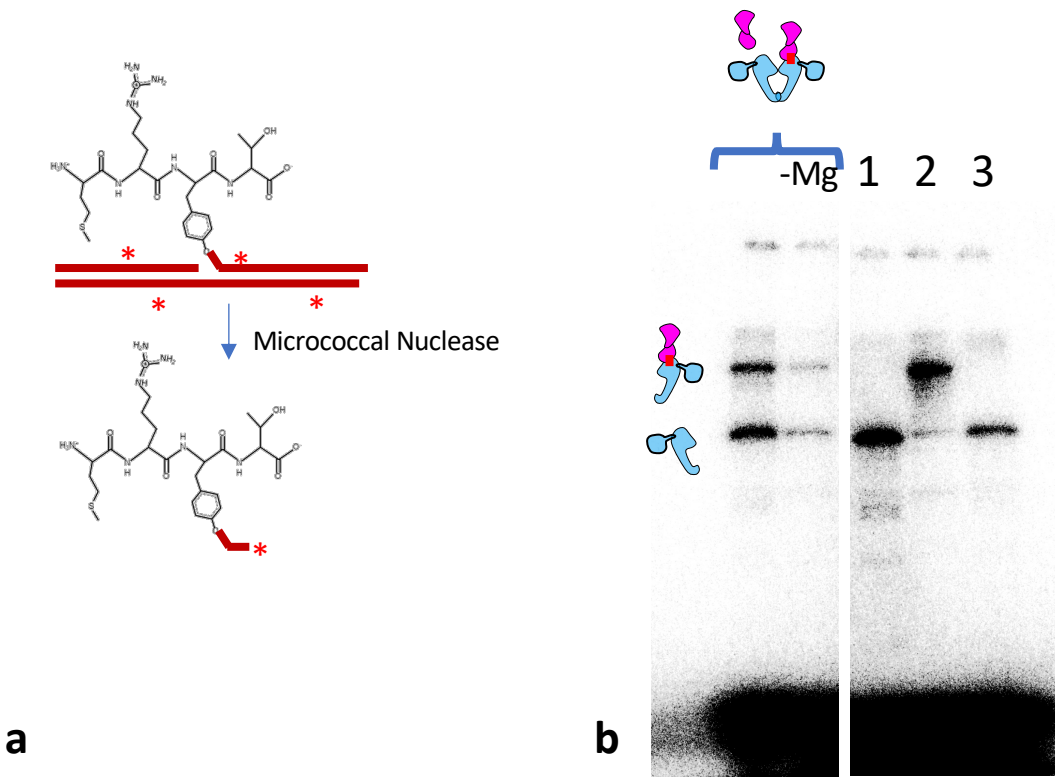

Figure 4

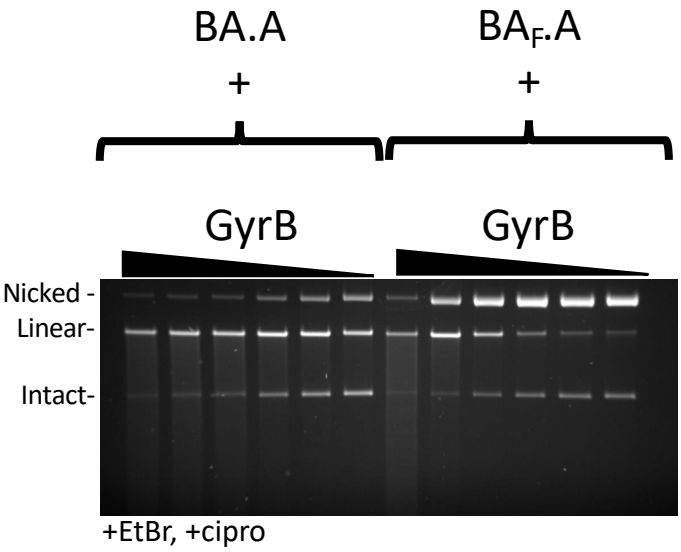

Figure 5

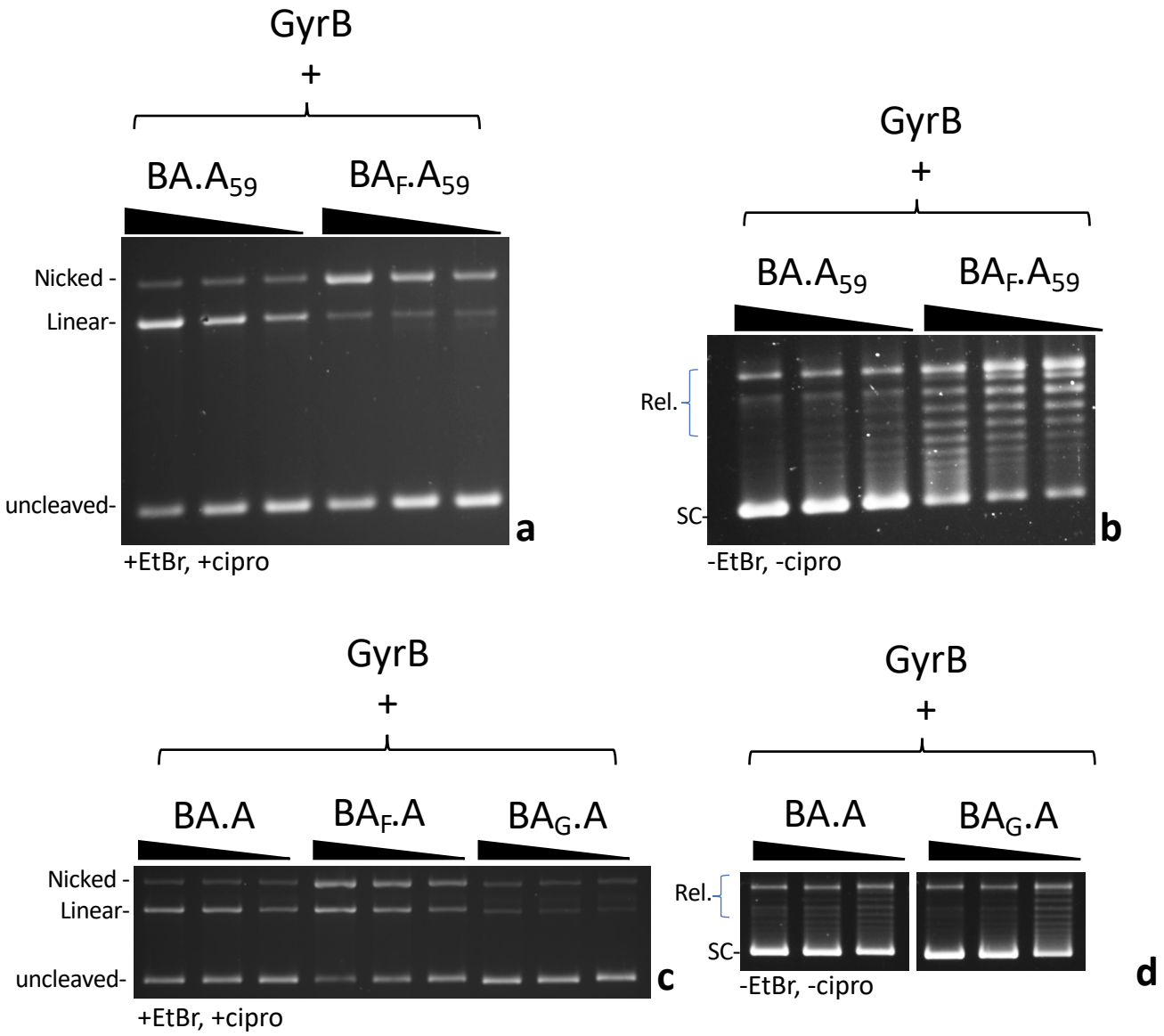
GyrB
+
BA.A59
BAF.A59
Nicked -
Linear-
uncleaved-
a
+EtBr, +cipro
GyrB
+
BA.A59
BAF.A59
Rel.
SC-
b
-EtBr, -cipro
GyrB
+
BA.A
BAF.A
BAG.A
Nicked -
Linear-
uncleaved-
c
+EtBr, +cipro
GyrB
+
BA.A
BAG.A
Rel.
SC-
-EtBr, -cipro
d

Figure 6

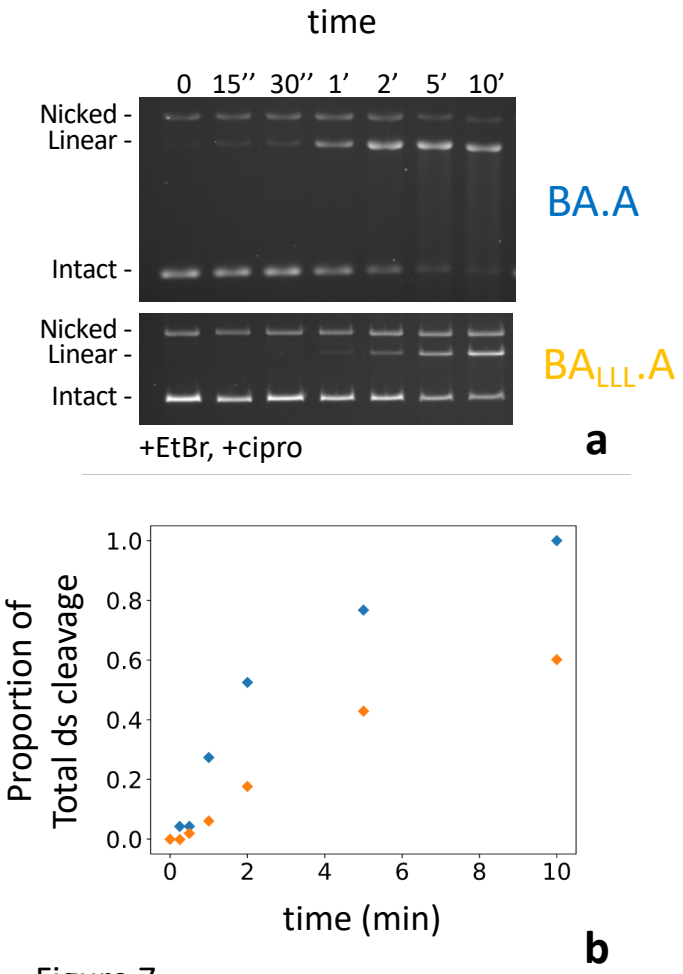
time
0 15'' 30'' 1' 2' 5' 10'
Nicked -
Linear -
Intact -
BA.A
Nicked -
Linear -
Intact -
BA$_{LLL}$.A
+EtBr, +cipro
a
Proportion of
Total ds cleavage
1.0
0.8
0.6
0.4
0.2
0.0
0
2
4
6
8
10
time (min)
b

Figure 7

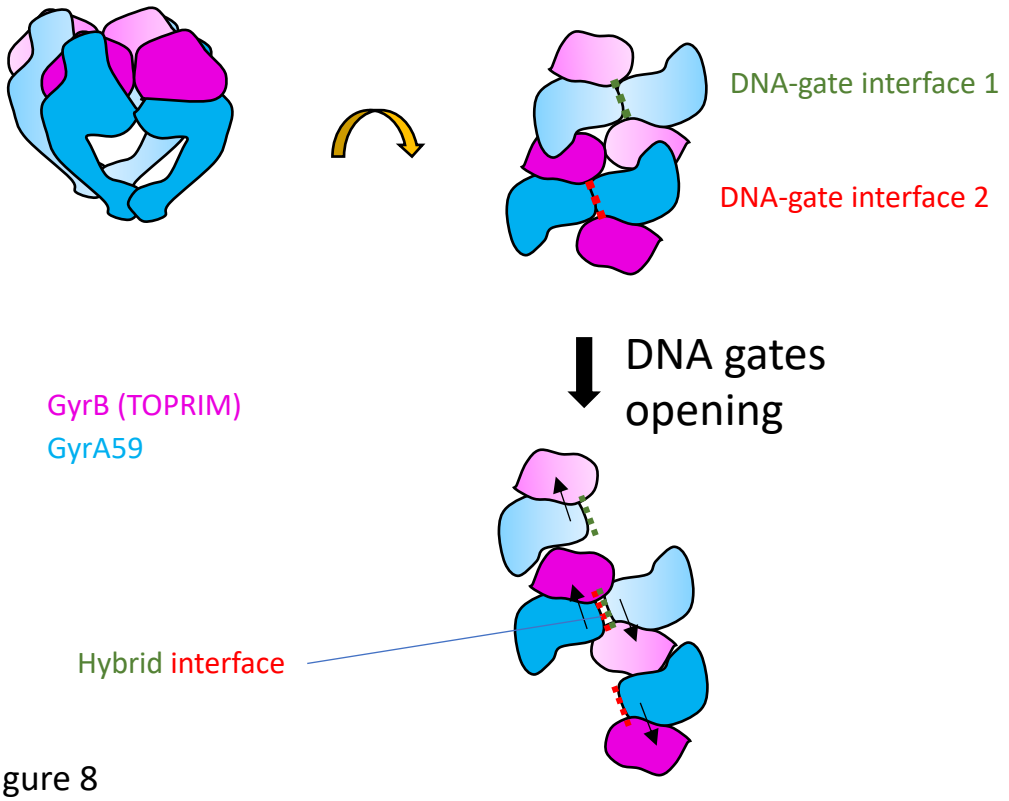
DNA-gate interface 1
DNA-gate interface 2
DNA gates opening
GyrB (TOPRIM)
GyrA59
Hybrid interface

Figure 8